Photochemistry and Photobiology, 2004, 80: 572–578

Effect of Carotenoids and Monogalactosyl Diglyceride on Bacteriochlorophyll *c* Aggregates in Aqueous Buffer: Implications for the Self-assembly of Chlorosomes¶

Pavel Klinger[1], Juan B. Arellano[2], František Vácha[3,4], Jan Hála[1] and Jakub Pšenčík*[1,4]

[1]Department of Chemical Physics and Optics, Faculty of Mathematics and Physics, Charles University, Prague, Czech Republic
[2]Instituto de Recursos Naturales y Agrobiología (CSIC), Salamanca, Spain
[3]Institute of Plant Molecular Biology, Academy of Sciences of the Czech Republic, České Budějovice, Czech Republic
[4]Institute of Physical Biology, University of South Bohemia, Nové Hrady, Czech Republic

Received 14 July 2004; accepted 22 September 2004

ABSTRACT

Aggregation of bacteriochlorophyll (BChl) *c* from chlorosomes, the main light-harvesting complex of green bacteria, has been studied in aqueous buffer. Unlike other chlorophyll-like molecules, BChl *c* is rather soluble in aqueous buffer, forming dimers. When BChl *c* is mixed with carotenoids (Car), the BChl *c* Q_y transition is further redshifted, in respect to that of monomers and dimers. The results suggest that Car are incorporated in the aggregates and induce further aggregation of BChl *c*. The redshift of the BChl *c* Q_y band is proportional to the Car concentration. In contrast, the mixture of bacteriochlorophyllide (BChlide) *c*, which lacks the nonpolar esterifying alcohol, does not form aggregates with Car in aqueous buffer or nonpolar solvents. Instead, the position of the BChlide *c* Q_y transition remains unshifted in respect to that of the monomeric molecule, and Car precipitates with the course of time in aqueous buffer. Similar effects on both BChl *c* and BChlide *c* are also observed when monogalactosyl diglyceride (MGDG), which forms the monolayer envelope of chlorosomes, is used instead of (or together with) Car. The results show that the hydrophobic interactions of the BChl *c* esterifying alcohols with themselves and the nonpolar carbon skeleton of Car, or the fatty acid tails of MGDG, are essential driving forces for BChl aggregation in chlorosomes.

INTRODUCTION

Bacteriochlorophyll (BChl) *c, d* and *e* are the major pigments found in the main light-harvesting complexes of green photosynthetic bacteria, the so-called chlorosomes (for a recent reviews see Blankenship and Matsuura [1] and Frigaard *et al.* [2]). A unique property of chlorosomes is that the main BChl pigments are not present in pigment–protein complexes, rather they form self-assembled aggregates based on their unusual chemical structure (3,4, review by Blankenship and Matsuura [1] and references therein). The main interactions involved in the formation of BChl aggregates are the coordination of the central Mg of a BChl molecule to a hydroxyethyl substituent at $C3^1$ of a neighboring BChl, which can be also hydrogen bonded to the keto group at $C13^1$ of a third BChl molecule (5,6). The aggregation leads to strong exciton interactions between BChl monomers, which in turn modulate optical properties of the BChl aggregates. Models, in which BChl pigments were organized into large rods, were proposed on the basis of freeze fracture electron microscopy and spectroscopic constraints (5–9). Recently a lamellar model, in which BChl molecules aggregate into semicrystalline lateral arrays, has been proposed (10). Aggregates with very similar optical properties to those in chlorosomes can be prepared *in vitro* either in nonpolar solvents or in aqueous buffers with addition of lipids (4,11, reviews by Blankenship and Matsuura [1] Blankenship *et al.* [12] and Tamiaki [13]).

Chlorosomes also contain carotenoids (Car) in amounts that depend on bacterial species, growth phase, and light and temperature conditions; thereby, the stoichiometry between BChl and Car varies between approximately 2:1 and 20:1 (14–17). In addition, the chlorosomal baseplate, which connects the chlorosome to the cytoplasmic membrane, contains monomeric BChl *a* in a pigment–protein complex together with the chlorosomal protein (Csm) A (1,18). Besides pigments, quinones are present in chlorosomes, acting as quenchers of excitation energy (19). The chlorosomal envelope consists of a glycolipid monolayer, mainly monogalactosyl diglyceride (MGDG), where other proteins of the Csm family are anchored in relatively small amounts, having seemingly no interaction with the BChl pigments.

The location and function of Car in chlorosomes is not yet well understood. A number of results indicate that one part of Car is present in the baseplate (20,21) and another part must be in close contact with chlorosomal BChl (22,23). The lamellar model provides plausible explanation for the location of 'chlorosomal' Car in the lipid-like space between the planes (10). The strong interaction between chlorosomal Car and BChl is also manifested by fast energy transfer from the S_2 state of Car to BChl (<100 fs^{-1})

¶Posted on the website on 15 October 2004.
*To whom correspondence should be addressed: Department of Chemical Physics and Optics, Faculty of Mathematics and Physics, Charles University, Ke Karlovu 3, 121 16 Prague 2, Czech Republic. Fax 420-221-911-249; e-mail: jakub.psencik@mff.cuni.cz

Abbreviations: BChl, bacteriochlorophyll; BChlide, bacteriochlorophyllide; Car, carotenoid; Csm, chlorosomal protein; HPLC, high-performance liquid chromatography; MGDG, monogalactosyl diglyceride.

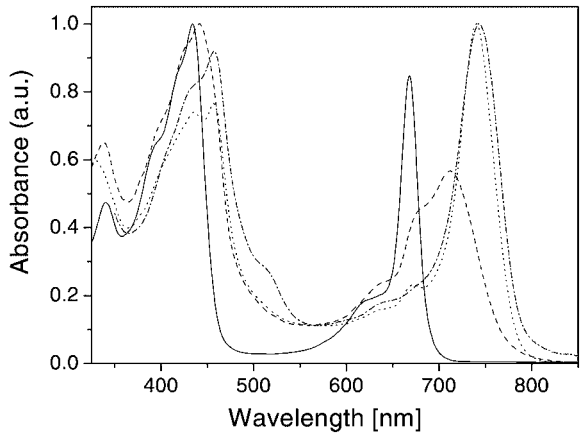

Figure 1. Absorption spectra of ~10 μ*M* BChl *c* in methanol (solid line), in 50 m*M* Tris–HCl pH 8.0 (dashed line) and mixed a priori with ~40 μ*M* MGDG and then dissolved in 50 m*M* Tris–HCl pH 8.0 (dotted line). The absorption spectrum of chlorosomes, containing also BChl *a* and Car, from *Chlorobium tepidum* is also shown for the sake of comparison (dash–dotted line).

(24) and by triplet–triplet energy transfer from BChl to Car (21,22,25), for which an overlap of electron wave functions is a prerequisite. Moreover, the amount of chlorosomal Car affects the optical spectra of BChl aggregates (23).

In this work we have studied the origin of the Car effect on the self-assembly of BChl *c* aggregates *in vitro* in aqueous buffer. We have used both BChl *c* and chlorobactene from the green sulfur bacterium *Chlorobium tepidum*. The results show that the chlorosomal BChl aggregation relies not only on the intermolecular interaction between the polar heads of BChl molecules but also on the hydrophobic interactions between the BChl esterifying alcohols themselves and between the BChl esterifying alcohol and the carbon skeleton of Car or the fatty acid tails of MGDG.

MATERIALS AND METHODS

Growth conditions. Growth culture media were initially inoculated with *Chlorobium tepidum* cells kindly gifted by Prof. G. Hauska (University of Regensburg, Germany). Cells were grown for 3 days at 48°C in modified Pfennig's medium (26) and stored at 4°C until use. Whole cells were harvested by centrifugation.

Bacteriochlorophyll c and carotenoids. BChl *c* and Car were extracted from whole cells of *Chlorobium tepidum* by means of acetone–methanol 7:2 (vol/vol). The mixture was centrifuged at high speed in a bench centrifuge and the supernatant collected. The pellet was newly suspended in the organic phase. Three cycles were enough to extract quantitatively all pigments. About 1 m*M* sodium ascorbate was added early to the whole cells to avoid pigment oxidation during the procedure. Phase separation by mixing the extracted pigments with light petroleum–dichloromethane 9:1 (vol/vol) and followed by 1 *M* NaCl was carried out to bring the bulk of pigments to the nonpolar epiphase. Pigments were dried under stream of nitrogen. A first crude separation between BChl *c*—main and secondary homologs—and Car—chlorobactene and its precursors—was achieved by washing out Car from the dried bulky film of pigments by hexane. Pigment fractions enriched in BChl *c* or Car were further purified by reverse phase high-performance liquid chromatography (HPLC) on a Tessek (Prague, Czech Republic) SGX C18 column 8 × 250 mm, particle size 7 μm using solvents A (100% methanol) and B (methanol–hexane 4:1, vol/vol) in a two-step gradient as follows: 100% solvent A for the first 10 min and 100% solvent B for the next 35 min. Each time, the column was (re)equilibrated with solvent A for 15 min before the next injection. The flow rate was 3 mL min^{-1}. The main four homologs of BChl *c*—esterified with farnesol—were collected in one single pool and so was chlorobactene with none of its derivatives.

Bacteriochlorophyllide c. Bacteriochlorophyllide *c* (BChlide *c*) was obtained by dissolving BChl *c* in 5% KOH methanol and left for 2 h at 30°C. BChlide *c* was further purified by reverse HPLC as described above, except that the flow rate was 1 mL min^{-1}. Both BChl *c* (Fig. 1) and BChlide *c* (not shown) have identical absorption spectra in methanol, but they differ from each other in HPLC retention time because of their significantly different polarity. All homologs of BChlide *c* were collected in one single pool. HPLC-purified pigments were dried under a stream of nitrogen and kept in an inert atmosphere at –20°C until use.

Preparation of BChl c aggregates. HPLC-purified BChl *c* was dissolved in methanol to a final concentration of approximately 3 m*M*; whereas HPLC-purified chlorobactene was in acetone (approximately 0.6 m*M*). A volume of 10 μL of BChl *c* in methanol was mixed with 0–10 μL of Car in acetone and the resulting mixture injected vigorously into 3 mL of 50 m*M* Tris–HCl pH 8.0. The final concentration of BChl *c* in buffer was approximately 10 μ*M*, and the concentration of Car varied between 0 and 2 μ*M*. Each sample was left on the bench for a few hours at room temperature and in dark so as to reach a steady-state absorption spectra, unless described in the text. When MGDG from Sigma (St. Louis, MO) was used, 0.1 mg of MGDG dissolved in 10 μL methanol was added to a mixture of BChl *c* and Car in methanol–acetone. The full mixture was then injected vigorously into 3 mL of 50 m*M* Tris–HCl pH 8.0 as described above. The maximal final concentration of MGDG was ~40 μ*M*.

Absorption spectra and determination of molecular concentrations. Absorption spectra were measured on Spectronic Unicam UV-300 (Cambridge, UK). The molar absorption coefficient of BChl *c* in methanol was determined to be 52 mM^{-1} cm^{-1} by comparing the absorption spectrum of BChl *c* dissolved in acetone (extinction coefficient 75.4 mM^{-1} cm^{-1}) (27) with the absorption spectrum of the same amount of BChl *c* redissolved in the same volume of methanol. The extinction coefficient of chlorobactene in acetone was determined to be 170 mM^{-1} cm^{-1} using the value of 161.7 mM^{-1} cm^{-1} for chlorobactene in light petroleum (recalculated from values given by Foppen [28]). For MGDG, a molar mass of 746 was used assuming esterification with one molecule of hexadecatrienoic acid (16:3) and another of γ-linolenic acid (18:3) (formula $C_{43}H_{70}O_{10}$).

RESULTS

BChl *c* is soluble in aqueous buffer

Figure 1 shows absorption spectra of BChl *c* in different environments. BChl *c* exists as a monomer for example in methanol (Q_y maximum at 669 nm). In chlorosomes, or when mixed with lipids (such as MGDG) and dissolved in aqueous buffers, the BChl *c* form aggregates with its Q_y absorption maximum peaking at ~740 nm. Surprisingly, pure BChl *c* is also soluble and stable in aqueous buffer. Its absorption spectrum is characterized by a main Q_y maximum at 710 nm and shoulders at ~635 nm and ~680 nm, *i.e.* very similar to that of BChl *c* dimers in nonpolar solvents (29) (see Discussion). To our knowledge, the solubility of pure BChl *c* in aqueous buffer was reported for the first time in the article by Uehara *et al.* (30), where Q_y absorption maxima of different BChl *c* homologs in phosphate buffer with and without MGDG are reported. The absorption spectra presented in this study correspond to the naturally occurring mixture of the four main homologs of BChl *c*.

Effect of Car on BChl *c* and BChlide *c* aggregation

To study the effect of Car on aggregation of BChl *c*, a series of samples with a constant concentration of BChl *c* and increasing concentrations of Car were prepared. Figure 2a shows the results of a typical experiment. Increasing concentration of Car led to pronounced changes in the absorption spectrum, mainly in the Q_y region of BChl *c*, where Car does not absorb. The main Q_y band underwent a redshift and an increase in intensity on increase in Car concentration, whereas the shoulders at ~635 and ~680 nm maintained their position but decreased in intensity. The actual Q_y

absorption maxima were at 730 nm (molar ratio BChl–Car 1:0.06), 735 nm (1:0.12) and 740 nm (1:0.18), not having further effect on the Q_y position ratios beyond the latter. The used stoichiometries between BChl *c* and chlorobactene were within a broad range as found in chlorosomes of several green photosynthetic bacteria (1:0.05–1:0.5) (16). The presence of Car in solution can be best monitored around 500 nm, where its contribution does not overlap with the Soret band of BChl *c*. The aggregates prepared from a mixture of BChl *c* and Car were stable for hours–days in dark at room temperature and Car did not precipitate. On attempting to dissolve only Car in aqueous buffer, Car completely precipitated in minutes–hours (not shown).

The results described above point to a fundamental interaction between Car and BChl *c*. To localize the site of the interaction, the same experiments were repeated using BChlide *c* instead of BChl *c* (Fig. 2b). BChlide *c*, which lacks the esterifying alcohol at $C17^3$, is by far a more polar molecule and, therefore, well soluble in aqueous buffers. In contrast to BChl *c*, the position of the BChlide *c* Q_y band (673 nm for all samples) was not affected by Car at all (Fig. 2b). Except for the redshift of the Q_y band from 669 to 673 nm, the absorption spectrum of BChlide *c* in aqueous buffer is very similar to that of BChlide *c* or BChl *c* in methanol, indicating that BChlide *c* remains as a monomer in aqueous buffer. This is also supported by the facts that BChlide *c* degrades into bacteriopheophorbide *c* within minutes–hours after preparation, and that the contribution of Car disappears from the absorption spectra on the same time scale as observed for pure Car in aqueous buffer, manifesting a lack of interaction with BChlide *c* (not shown).

In contrast to BChl *c*, BChlide *c* does not seem to form either dimers or aggregates even in organic solvents (polar or nonpolar) such as CH_2Cl_2 or hexane, according to the absorption spectra (Fig. 2b, inset). On top of this, when first BChl *c* is dissolved in organic solvents such as acetone, where it remains as a monomeric molecule, and second when the solvent is dried under a stream of nitrogen, dimers are formed as revealed by absorption spectroscopy. In contrast, the absorption spectrum of dried films of BChlide *c* (not shown) resembles that of monomeric BChlide *c* (Fig. 2b). This result shows that the inability of BChlide *c* to form aggregates is not just due to a solvent polarity effect but also due to the missing esterifying alcohol.

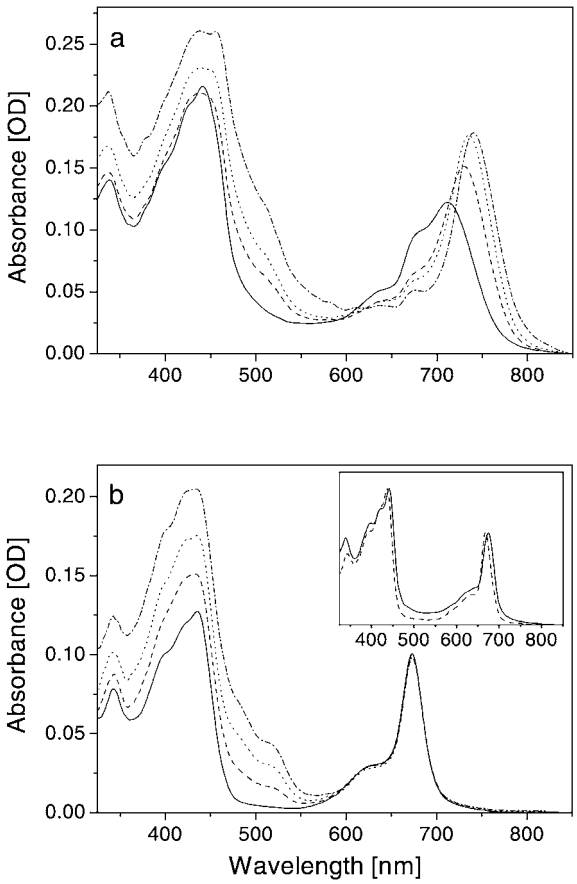

Figure 2. (a) Absorption spectra of BChl *c* in aqueous buffer with four different Car concentrations. Molecular ratios between BChl *c* and Car were 1:0 (solid line), 1:0.06 (dashed line), 1:0.12 (dotted line) and 1:0.18 (dash–dotted line). (b) BChlide *c* in aqueous buffer with four different Car concentrations. Molecular ratios between BChlide *c* and Car were the same as in (a). The spectra were recorded shortly after preparation. The inset shows normalized absorption spectra of BChlide *c* in hexane-$CHCl_3$ (200:1 vol/vol, solid line) and CH_2Cl_2–$CHCl_3$ (200:1 vol/vol, dashed line).

Effect of MGDG on BChl *c* and BChlide *c* in aqueous buffer

BChl *c, d* or *e* aggregates in aqueous buffers are usually prepared in the presence of lipids, *e.g.* MGDG (30) or lecithin (31), inducing the aggregation. Figure 3 summarizes the results of experiments carried out to explore the interaction of MGDG with BChl *c*. On adding MGDG up to a final concentration of approximately 0.003% to the mixture of BChl *c* and Car, a constant shift of the BChl *c* Q_y band for all samples was observed, no matter what the Car concentration was (Fig. 3a). The used concentration of MGDG was previously reported to saturate the bathochromic shift of BChl *c* aggregates in aqueous buffer (30), and Car thus cannot induce any further redshift (BChl *c*–Car–MGDG ratios were between 1.0:0–0.2:4.0 in this study). Nevertheless, Car were intriguingly stabilized inside the aggregates and did not precipitate (Fig. 3a). The absorption spectra of these aggregates resemble that of chlorosomes (Fig. 1). An addition of Car at different concentrations to BChl *c* aggregates, prepared several hours before in the presence of MGDG, has no effect on the absorption spectra and Car precipitated soon. This suggests that Car does not get inside the aggregates once they have formed. A similar effect was also observed, when a mixture of BChl *c* and Car was first injected to the aqueous buffer and MGDG up to 0.003% was added afterward. In this case the absorption spectra of BChl *c* and Car (Fig. 2a) also remained unaffected (not shown). These results indicate that aggregates are formed after injection, and further additions do not change them.

Using increasing concentrations of MGDG (from 0 to 0.003%), the BChl *c* Q_y band gradually shifts to the red (Fig. 3b) in agreement with previous results (30). Interestingly, the effects of both MGDG and Car are complementary: The large redshift (Q_y peak at ~740 nm) can be obtained also by mixing nonsaturating concentrations of MGDG and Car, which would not be sufficient to reach the full redshift if used separately (not shown). In addition, the effect of MGDG on the absorption spectrum of BChlide *c* was investigated; however, no shift of the BChlide *c* Q_y band was observed (not shown), suggesting that MGDG does not interact or does not induce aggregation of BChlide *c* similar to Car.

All these results suggest that the interaction leading to the redshift of the BChl *c* Q_y band in the presence of Car or MGDG (or both) is similar. However, it is expected that there might be differences between the two types of BChl *c* aggregates. One

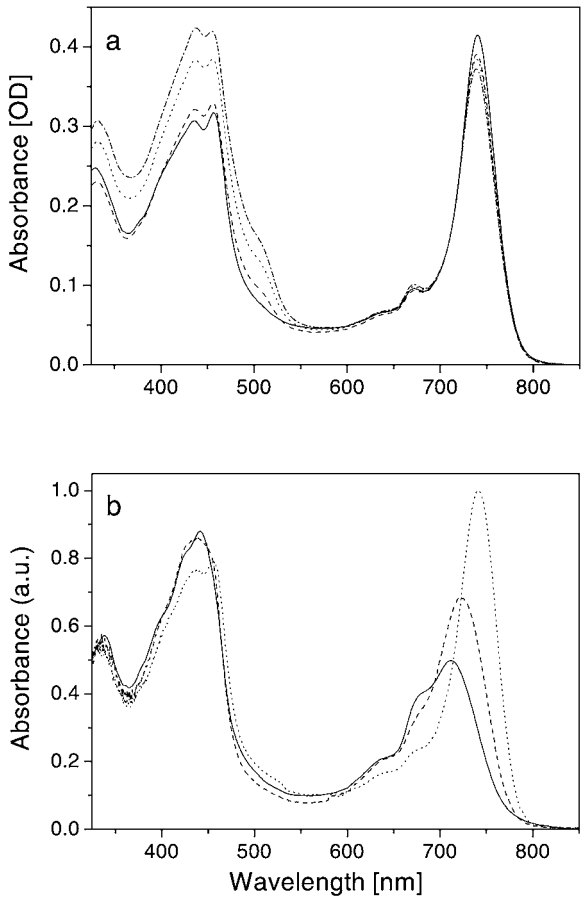

Figure 3. (a) Absorption spectra of MGDG BChl *c* aggregates in aqueous buffer with four different Car concentrations. Molecular ratios between BChl, Car and MGDG were 1:0:4 (solid line), 1:0.06:4 (dashed line), 1:0.12:4 (dotted line) and 1:0.18:4 (dash–dotted line). (b) Absorption spectra of MGDG BChl *c* aggregates in aqueous buffer with three different MGDG concentrations. Molecular ratios between BChl *c* and MGDG were 1:0 (solid line), 1:1 (dashed line) and 1:4 (dotted line). Spectra are normalized to equal absorbed energy.

difference that can be drawn easily on comparing the absorption spectra of Figs. 2a and 3a is that there is less light scattering in the MGDG-induced BChl *c* aggregates than in the Car-induced ones, indicating that the former aggregates have a smaller size.

DISCUSSION

Pure BChl *c* form dimers in aqueous buffer

Despite the fact that chlorophyll-like molecules have a polar tetrapyrrole head, they are scarcely soluble in aqueous buffers, because of their nonpolar esterifying alcohol tails at $C17^3$. On removing the tails, the solubility of their corresponding (B)Chlide changes remarkably, being thus easily soluble in aqueous buffers. Conversely, (B)Chl are soluble in polar organic solvents. BChl *c*, as does BChlide *c*, exists as a monomer, *e.g.* in methanol, where the central Mg ion is known to be six coordinated (32 and references therein). The absorption spectra of BChlide *c* in methanol and aqueous buffer are very similar, suggesting that BChlide *c* also exists as a monomer in aqueous buffers.

In contrast to other nonchlorosomal (B)Chl molecules, BChl *c* is rather soluble in aqueous buffer (Fig. 1), but its absorption spectrum clearly differs from that of monomeric BChl *c* in methanol or BChlide *c* in methanol or aqueous buffer. The overall shape of the absorption spectrum, including positions and relative intensities of all three bands and shoulders in the Q_y region of BChl *c* in aqueous buffer, fits very well with the absorption spectra of 2 m*M* BChl *c* in CCl_4 and benzene, and especially in CH_2Cl_2. In the former two solvents, BChl *c* form stable antiparallel dimers with a piggyback conformation, whose structure was determined by nuclear magnetic resonance (29,33,34). In solvents with higher polarity (CH_2Cl_2), antiparallel dimers may coexist with the so called T-dimers, where one of the central Mg ions of BChl *c* is not coordinated to the hydroxyethyl group at $C3^1$ of the neighboring BChl *c*. This situation is likely to occur in aqueous buffer because the latter group has to compete with hydroxyl groups of the water bulk for the central Mg ion. So both, antiparallel and T-shaped dimers of BChl *c* could thus coexist in aqueous buffer. To confirm that BChl *c* form dimers in aqueous buffer, which might be the building block of higher aggregates, Raman and proton nuclear magnetic resonance spectroscopies are planned to be used in the near future.

In addition, BChl *c* molecules are strikingly stable in aqueous buffer and do not degrade as easy as monomeric BChl *c* or BChlide *c* in solution. The increased stability of BChl *c* dimers and higher aggregates might be explained, for example, by their drastically decreased quantum yield of triplet state population (compared with monomers) and consequently of singlet oxygen sensitization (35,36) as a result of a shorter singlet lifetime. Another reason for the increased stability of aggregates is that the coordination of Mg of one BChl molecule to the hydroxyethyl substituent at $C3^1$ of a neighboring BChl stabilizes the Mg ion and prevents pheophytization.

Car and MGDG interact with BChl *c* via its esterifying alcohol

Our results show unambiguously that nonpolar Car, such as chlorobactene, directly interact with BChl *c* in aqueous buffer. This interaction enables Car to remain dissolved in buffer and intriguingly affects the absorption spectra of BChl *c* dimers in their Q_y spectral region, where Car do not absorb. An important matter is to know the mechanism behind this interaction. Because neither stabilization nor interaction of Car in aqueous buffer is observed when BChlide *c* is used instead of BChl *c*, it is thus plausible to explain stabilization of Car in aqueous buffer by hydrophobic interaction with the soluble BChl *c* dimers via the carbon skeleton of Car and the nonpolar esterifying alcohol tail of BChl *c*. The effect of Car on BChl *c* spectra, namely the observed redshift, can be explained either by the decreased polarizability of the BChl *c* local environment by the presence of Car or by the buildup of larger aggregates from BChl *c* dimers induced by Car, which would lead to new excitonic interactions between the BChl *c* molecules. The former possibility is less likely because it is known that the shift of the Q_x and Soret bands is solvent dependent, whereas the shift of the Q_y band is usually less significant (37). Moreover, the effect of solvents with different polarizability on the position of the Q_y transition was evaluated: BChl *c* and BChlide *c* were dissolved in hexane (refractive index n = 1.375; polarizability $(n^2 - 1)/(n^2 + 2) = 0.229$) and in tetradecane (refractive index 1.429, polarizability 0.258). Interestingly, the peak position of the BChlide *c* Q_y was at 674 nm in both cases, showing no dependence on polarizability and no indication of aggregation, in contrast to

BChl *c* (not shown). Therefore, the possibility that Car induces formation of larger aggregates seems to be more reasonable, which is also supported by the fact that the final absorption spectra of BChl *c* aggregates in the presence of Car resemble those of chlorosomes, where large aggregates of BChl *c* are present.

The effect of MGDG on the absorption spectra of BChl *c* was similar to that of Car. The hydrophobic interaction between the BChl *c* esterifying alcohol and the MGDG esterifying acid tails is expected to be the driving force for the BChl *c* aggregation also in this case. It is well documented that artificial MGDG aggregates of BChl *c* can be formed with no need of proteins or Car in aqueous buffer, reaching absorption and circular dichroism spectra very similar to those of chlorosomes (11,30,38). It is assumed that in artificial MGDG aggregates, a monolayer of MGDG surrounds the BChl *c* aggregates as in chlorosomes, forming a hydrophobic interior, which favors the intermolecular interaction among BChl. A lack of such an envelope in BChl–Car aggregates may lead to a tendency to form larger complexes, which explains the observed larger scattering of the Car–BChl aggregates.

In contrast to BChl *c*, we did not find any evidence that BChlide *c* forms either dimers or aggregates in aqueous buffer, CH_2Cl_2 or hexane. This indicates that the hydrophobic interaction between the esterifying alcohols is essential, as a first step, for the formation of dimers of BChl *c*. This hydrophobic interaction is also manifested in dried films of BChl *c*, ruling out that the polarity (or the polarizability) of the solvent is the reason behind the failure of BChlide *c* to form dimers.

In summary, formation of aggregates with absorption spectra similar to those in chlorosomes can be induced by addition of either Car or MGDG, or both. In both cases, the hydrophobic interaction between the esterifying alcohol of BChl *c* and either the Car skeleton or MGDG fatty acids, as well as the interaction between esterifying alcohols themselves, plays an essential role. Figure 4 shows the principles of the proposed interactions. These hydrophobic interactions seem to be the driving force for the overall assembly of monomers to dimers and into larger aggregates. The results support a recently proposed model for the chlorosome structure (10), in which undulated planar BChl aggregates form lamellar structures through the interaction between interdigitated esterifying alcohol tails of neighboring planes. Car are localized in the lipid-like space between the lamellar planes. The hydrophobic interactions are responsible for maintaining the lamellar organization and the stabilization of Car in the aggregate structure, in agreement with the results presented here. Car thus play mainly a structural role and have a direct effect on the position of the Q_y band of BChl aggregates in chlorosomes, in addition to the photoprotective and light-harvesting functions (20,24). To our knowledge, the described hydrophobic interactions have not been taken into account in previous models based on rod elements. In addition, planar aggregates are formed through the specific interactions of the chlorin rings (see Introduction), which represent the other category of interactions that are unambiguously essential for the chlorosome assembly too.

Although the hydrophobic interaction with esterifying alcohols of BChl *c* is common for MGDG and Car, the role of MGDG and Car has subtle differences. MGDG seems to be essential to create the hydrophobic environment that is necessary for an optimal shape and size of the overall aggregate complex. These MGDG-induced artificial aggregates of BChl *c* are of similar dimensions as chlorosomes (38). On the contrary, Car stabilize themselves inside the hydrophobic space between the chlorin rings and induce the formation of large aggregates by strengthening the hydrophobic interaction between BChl *c* dimers. By creating a more hydrophobic microenvironment around BChl *c*, Car can also help convert T-shaped dimers into antiparallel dimers, which might be the building block of the BChl *c* aggregates (6,10,33,39–41; other authors suggest parallel monomers as the building block, see van Rossum *et al*. [9] and references therein) and thus enlarge the aggregation order of BChl *c*. In addition, a possible π–π interaction between the Aryl end group of chlorobactene and the chlorin ring can ensure the overlap of electron wave functions, which is a necessary prerequisite for the triplet–triplet energy transfer.

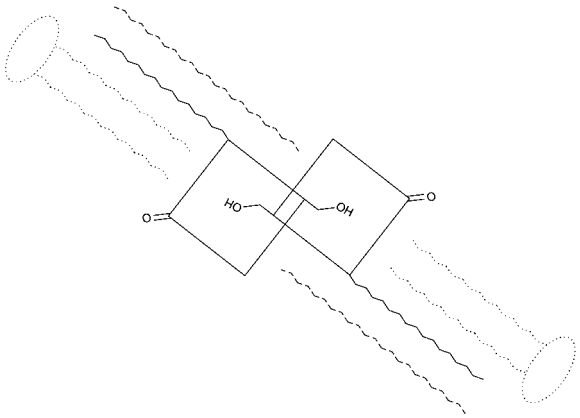

Figure 4. Simplified scheme of the proposed interactions between BChl *c* (solid line), Car (dashed line) and MGDG (dotted line). BChl is shown in a dimeric form, which can be extended into a larger aggregate by hydrogen bonding to another dimer to the left and right and by chlorin stacking in the direction above and below the plane of paper.

Finally, it is worth noting that all the trends described here are very well reproducible, with pigments from bacteria grown at different conditions; however, the actual positions and intensities of particular absorption bands may differ.

CONCLUSIONS

Pure BChl *c* forms dimers in aqueous buffers. The interaction between the esterifying alcohols is an essential driving force in this process, together with the well-known hydrogen bonding and Mg coordination net between the chlorin rings. Car and MGDG interact directly with BChl *c* via hydrophobic interaction with the esterifying alcohol tail of BChl *c* and possibly diminish solvation around the BChl *c* head. Interaction of BChl *c* with Car induces self-assembly of the BChl *c* dimers into large aggregates with Car incorporated into the aggregate structure. These large aggregates have chlorosome-like absorption spectra, similar to MGDG-induced BChl aggregates. The results have an important consequence for the understanding of the BChl self-assembly in chlorosomes and for the preparation of artificial BChl aggregates with defined properties. Further, these findings support a recently proposed lamellar model for the organization of BChl *c* aggregates in chlorosomes, which relies on the hydrophobic interactions between esterifying alcohols of BChl *c* molecules from neighboring planes (10). Also, the model and the results presented here predict that chlorosomal Car are stabilized in the hydrophobic space between the planes.

Acknowledgements—The authors express their gratitude to Prof. G. Hauska (University of Regensburg, Germany) for providing *Chlorobium tepidum*

cells. This work was supported by the Czech Science Foundation and Czech Ministry of Education, Youth and Sports (contracts 206/02/0942, LN00A141). J.B.A. is very grateful to the CSIC Marina Bueno program and the Spanish Ministry of Science and Technology for financial support (project reference AGL2003-00045).

REFERENCES

1. Blankenship R. E. and K. Matsuura (2003) Antenna complexes from green photosynthetic bacteria. In *Light-harvesting Antennas* (Edited by B. R. Green and W. W. Parson), pp. 195–217. Kluwer Academic Publishers, Dordrecht, The Netherlands.
2. Frigaard, N. U., A. G. M. Chew, H. Li, J. A. Maresca and D. A. Bryant (2003) *Chlorobium tepidum*: insights into the structure, physiology, and metabolism of a green sulfur bacterium derived from a complete genome sequence. *Photosynth. Res.* **78**, 93–117.
3. Krasnovsky, A. A. and E. V. Pakshina (1959) The photochemical and spectral properties of bacterioviridin of green sulfur bacteria. *Dokl. Akad. Nauk. SSSR* **127**, 215–218. [English Translation]
4. Bystrova, M. I., I. N. Mal'gosheva and A. A. Krasnovsky (1979) Study of molecular mechanism of self-assembly of aggregated forms of bacteriochlorophyll *c*. *Mol. Biol.* **13**, 440–451.
5. Holzwarth, A. R. and K. Schaffner (1994) On the structure of bacteriochlorophyll molecular aggregates in the chlorosomes of green bacteria. A molecular modelling study. *Photosynth. Res.* **41**, 225–233.
6. Nozawa, T., K. Ohtomo, M. Suzuki, H. Nakagawa, Y. Shikama, H. Konami and Z. Y. Wang (1994) Structures of chlorosomes and aggregated BChl *c* in *Chlorobium tepidum* from solid state high resolution CP/MAS ^{13}C NMR. *Photosynth. Res.* **41**, 211–233.
7. Staehelin, L. A., J. R. Golecki, R. C. Fuller and G. Drews (1978) Visualization of the supramolecular architecture of chlorosome (Chlorobium type vesicles) in freeze-fractured cells of *Chloroflexus aurantiacus*. *Arch. Microbiol.* **119**, 269–277.
8. Staehelin, L. A., J. R. Golecki and G. Drews (1980) Supramolecular organization of chlorosome (Chlorobium vesicles) and of their membrane attachment site in *Chlorobium limicola*. *Biochim. Biophys. Acta* **589**, 30–45.
9. van Rossum, B. J., D. B. Steensgaard, F. M. Mulder, G. J. Boender, K. Schaffner, A. R. Holzwarth and H. M. de Groot (2001) A refined model of the chlorosomal antennae of the green bacterium *Chlorobium tepidum* from proton chemical shift constraints obtained with high-field 2-D and 3-D MAS NMR dipolar correlation spectroscopy. *Biochemistry* **40**, 1587–1595.
10. Psencik, J., T. P. Ikonen, P. Laurinmäki, M. C. Merckel, S. J. Butcher, R. E. Serimaa and R. Tuma (2004) Lamellar organization of pigments in chlorosomes, the light harvesting complexes of green photosynthetic bacteria. *Biophys. J.* **87**, 1165–1172.
11. Hirota, M., T. Moriyama, K. Shimada, M. Miller, J. M. Olson and K. Matsuura (1992) High degree of organization of bacteriochlorophyll *c* in chlorosome-like aggregates spontaneously assembled in aqueous solution. *Biochim. Biophys. Acta* **1099**, 271–274.
12. Blankenship, R. E., J. M. Olson and M. Miller (1995) Antenna complexes from green photosynthetic bacteria. In *Anoxygenic Photosynthetic Bacteria* (Edited by R. E. Blankenship, M. T. Madigan and C. E. Bauer), pp. 399–435. Kluwer Academic Publishers, Dordrecht, The Netherlands.
13. Tamiaki, H. (1996) Supramolecular structure in extramembraneous antennae of green photosynthetic bacteria. *Coord. Chem. Rev.* **148**, 183–197.
14. Liaaen-Jensen, S. (1965) Bacterial carotenoids. XVIII. Aryl carotenoids from *Phaeobium*. *Acta Chem. Scand.* **19**, 1025–1030.
15. Schmidt, K. (1980) A comparative study on the composition of chlorosomes (*Chlorobium* vesicles) and cytoplasmic membranes from *Chloroflexus aurantiacus* OK-70-fl and *Chlorobium limicola* f. *thiosulfatophilum* strain 6230. *Arch. Microbiol.* **124**, 21–31.
16. Borrego, C. M. and L. J. Garcia-Gil (1995) Rearrangement of light harvesting bacteriochlorophyll homologues as a response of green sulfur bacteria to low light intensities. *Photosynth. Res.* **45**, 21–30.
17. Oelze J. and J. R. Golecki (1995) Membranes and chlorosomes of green bacteria: Structure, composition, and development. In *Anoxygenic Photosynthetic Bacteria* (Edited by R. E. Blankenship, M. T. Madigan and C. E. Bauer), pp. 259–278. Kluwer Academic Publishers, Dordrecht, The Netherlands.
18. Montaño, G. A., H. M. Wu, S. Lin, D. C. Brune and R. E. Blankenship (2003) Isolation and characterization of the B798 light-harvesting baseplate from the chlorosomes of *Chloroflexus aurantiacus*. *Biochemistry* **42**, 10246–10251.
19. Frigaard, N. U., S. Takaichi, M. Hirota, K. Shimada and K. Matsuura (1997) Quinones in chlorosomes of green sulfur bacteria and their role in the redox-dependent fluorescence studied in chlorosome-like bacteriochlorophyll *c* aggregates. *Arch. Microbiol.* **167**, 343–349.
20. Arellano, J. B., T. B. Melø, C. M. Borrego, J. Garcia-Gil and K. R. Naqvi (2000) Nanosecond laser photolysis studies of chlorosomes and artificial aggregates containing bacteriochlorophyll *e*: evidence for the proximity of carotenoids and bacteriochlorophyll *a* in chlorosomes from *Chlorobium phaeobacteroides* strain CL1401. *Photochem. Photobiol.* **72**, 669–675.
21. Carbonera, D., E. Bordignon, G. Giacometti, G. Agostini, A. Vianelli and C. Vannini (2001) Fluorescence and absorption detected magnetic resonance of chlorosomes from green bacteria *Chlorobium tepidum* and *Chloroflexus aurantiacus*. A comparative study. *J. Phys. Chem. B* **105**, 246–255.
22. Psencik, J., G. F. W. Searle, J. Hala and T. J. Schaafsma (1994) Fluorescence-detected magnetic-resonance (FDMR) of green sulfur photosynthetic bacteria *Chlorobium* sp. *Photosynth. Res.* **40**, 1–10.
23. Arellano, J. B., J. Psencik, C. M. Borrego, Y. Z. Ma, R. Guyoneaud, J. Garcia-Gil and T. Gillbro (2000) Effect of carotenoid biosynthesis inhibition on the chlorosome organization in *Chlorobium phaeobacteroides* strain CL1401. *Photochem. Photobiol.* **71**, 715–723.
24. Psencik, J., Y. Z. Ma, J. B. Arellano, J. Garcia-Gil, A. R. Holzwarth and T. Gillbro (2002) Excitation energy transfer in chlorosomes of *Chlorobium phaeobacteroides* strain CL1401: the role of carotenoids. *Photosynth. Res.* **71**, 5–18.
25. Melø, T. B., N. U. Frigaard, K. Matsuura and K. R. Naqvi (2000) Electronic energy transfer involving carotenoid pigments in chlorosomes of two green bacteria: *Chlorobium tepidum* and *Chloroflexus aurantiacus*. *Spectrochim. Acta A Mol. Biomol. Spectrosc.* **56**, 2001–2010.
26. Wahlund, T. M., C. R. Woese, R. W. Castenholz and M. T. Madigan (1991) A thermophilic green sulfur bacterium from New Zealand hot-springs, *Chlorobium tepidum* sp. nov. *Arch. Microbiol.* **156**, 81–90.
27. Oelze, J. (1985) Analysis of bacteriochlorophylls. *Methods Microbiol.* **18**, 257–284.
28. Foppen, F. H. (1971) Tables for identification of carotenoid pigments. *Chromatogr. Rev.* **14**, 133–298.
29. Umetsu, M., R. Seki, T. Kadota, Z. Y. Wang, T. Adschiri and T. Nozawa (2003) Dynamic exchange properties of the antiparallel bacteriochlorophyll *c* dimers. *J. Phys. Chem. B* **107**, 9876–9882.
30. Uehara, K., M. Mimuro, Y. Ozaki and J. M. Olson (1994) The formation and characterization of the in-vitro polymeric aggregates of bacteriochlorophyll *c* homologs from *Chlorobium limicola* in aqueous suspension in the presence of monogalactosyl diglyceride. *Photosynth. Res.* **41**, 235–243.
31. Steensgaard, D. B., H. Wackerbarth, P. Hildebrandt and A. R. Holzwarth (2000) Diastereoselective control of bacteriochlorophyll *e* aggregation. 3(1)-S-BChl *e* is essential for the formation of chlorosome-like aggregates. *J. Phys. Chem. B* **104**, 10379–10386.
32. Umetsu, M., Z. Y. Wang, M. Kobayashi and T. Nozawa (1999) Interaction of photosynthetic pigments with various organic solvents—magnetic circular dichroism approach and application to chlorosomes. *BBA Bioenergetics* **1410**, 19–31.
33. Wang, Z. Y., M. Umetsu, M. Kobayashi and T. Nozawa (1999) Complete assignment of H^1 NMR spectra and structural analysis of intact bacteriochlorophyll *c* dimer in solution. *J. Phys. Chem. B* **103**, 3742–3753.
34. Umetsu, M., R. Seki, Z. Y. Wang, I. Kumagai and T. Nozawa (2002) Circular and magnetic circular dichroism studies of bacteriochlorophyll *c* aggregates: T-shaped and antiparallel dimers. *J. Phys. Chem. B* **106**, 3987–3995.
35. Krasnovsky, A. A., J. Lopez, P. Cheng, P. A. Liddell, R. E. Blankenship, T. A. Moore and D. Gust (1994) Generation and quenching of singlet molecular oxygen by aggregated bacteriochlorophyll *d* in model systems and chlorosomes. *Photosynth. Res.* **40**, 191–198.
36. Arellano, J. B., T. B. Melø, C. A. Borrego and K. R. Naqvi (2002) Bacteriochlorophyll *e* monomers, but not aggregates, sensitize singlet oxygen: implications for a self-protection mechanism in chlorosomes. *Photochem. Photobiol.* **76**, 373–380.
37. Linnanto, J. and J. Korppi-Tommola (2001) Spectroscopic properties of Mg-chlorin, Mg-bacteriochlorin, and bacteriochlorophylls *a, b, c, d, e, f,*

g, and *h* studied by semiempirical and *ab initio* MO/CI methods. *J. Phys. Chem. A* **105**, 3855–3866.
38. Miller, M., T. Gillbro and J. M. Olson (1993) Aqueous aggregates of bacteriochlorophyll *c* as a model for pigment organization in chlorosomes. *Photochem. Photobiol.* **57**, 98–102.
39. Umetsu, M., Z. Y. Wang, J. Zhang, T. Ishii, K. Uehara, Y. Inoko, M. Kobayashi and T. Nozawa (1999) How the formation process influences the structure of BChl *c* aggregates. *Photosynth. Res.* **60**, 229–239.
40. Mizoguchi, T., K. Hara, H. Nagae and Y. Koyama (2000) Structural transformation among the aggregate forms of bacteriochlorophyll *c* as determined by electronic-absorption and NMR spectroscopies: dependence on the stereoisomeric configuration and on the bulkiness of the 8-C side chain. *Photochem. Photobiol.* **71**, 596–609.
41. Frese, R., U. Oberheide, I. H. M. van Stokkum, R. van Grondelle, M. Foidl, J. Oelze and H. van Amerongen (1997) The organization of bacteriochlorophyll *c* in chlorosomes from *Chloroflexus aurantiacus* and the structural role of carotenoids and protein—an absorption, linear dichroism, circular dichroism and Stark spectroscopy study. *Photosynth. Res.* **54**, 115–126.